Remaining Life of Fastener Joints Under Bearing and Bypass Fatigue Loading

I. Syed, B. Dattaguru, and A. R. Upadhya

Abstract Fastener joints are the desired joining techniques in many engineering applications since they make a rapid method to assemble and disassemble large structures. However, these joints are often susceptible to stress concentrations at critical locations due to their geometry with discontinuities. With further usage under fatigue loading, damage initiates and grows to a critical value at these locations affecting the integrity of the structure. Numerical analysis is carried out to study the stress variations in the plate-hole boundary of lap joint with fasteners accounting for different bearing and bypass loads ratios. The damage severity is studied under different R-ratios when subjected to FALSTAFF loading where the four-point rainflow cycle counting is used to extract the number of cycles. Damage growth is assessed by Paris' law with Elber correction factor wherein the fracture parameters are computed using MVCCI formulation. This approach helps in estimating the remaining life of the joint at any given operational conditions which in turn assists in the development of a computational model to build a digital twin for structural joints.

Keywords Fasteners · Bearing and bypass load · MVCCI

List of symbols

a	Material constants in Paris' law
C and m	Crack length
$G_{I:}$ Mode I	strain energy release rate (SERR)
K_{IC}	Mode I fracture toughness
σ_a	Applied load in the form of UDL
e	Distance to the centre of hole from right support
P_f	Bypass load
U_0	Imposed displacement at right end
R_P	Load ratio $= \frac{P_{\min}}{P_{\max}}$

I. Syed (✉) · B. Dattaguru · A. R. Upadhya
School of Aerospace Engineering, Jain (Deemed-To-Be University), Bengaluru, India

K. Jonnalagadda et al. (eds.), *Advances in Structural Integrity*, Lecture Notes in Mechanical Engineering, https://doi.org/10.1007/978-981-16-8724-2_19

$\sigma_{\theta\theta}$	Tangential stress
$a^{'}$ and $b^{'}$	Material constants in Elber's crack growth model
E and v	Young's modulus and Poisson's ratio
K_I	Mode I stress intensity factor (SIF)
N	Number of cycles
P_b	Bearing load at pin
P_a	Total applied load
$K_{\max}$ and $K_{\min}$	Maximum and minimum SIF
P_b/P_{f}	Bearing-bypass load ratio

1 Introduction

Fastener joints are widely used in aircrafts to connect different parts in primary and secondary structures. These create a non-permanent joint, unlike the case of welded or adhesive bonds and also allow easy assembly and dismantling [1]. However even though fastener joints provide easy access to inspect, they pose the problem of stress concentrations and are susceptible to damages such as cracks under operational conditions. Such cracks could grow to the critical sizes under aircraft flight loads during service life. It becomes necessary that such a fastener joint is analysed suitably to ensure safety. Research has been carried out both experimentally and numerically on fastener joints in both metallic as well as composite structures to estimate the strength of the joints under varying bearing to bypass loading ratios [2, 3, 13]. Considerable work has been done on both metallic and composite joints before 2010. Whereas in the past decade most of the work is carried out on multi-fastener composites joints. Recent work involving a metallic joint under fatigue loading to predict remaining life is scanty. Prediction of joint strength using numerical methods has been carried out on multi-fastener composite joints [7] by considering effects of bypass load and the results are compared with existing experimental work. An experimental investigation on fatigue crack growth behaviour in composites has been carried out [14] by considering pin loading effects and bypass load and it was found that the pin loading dominates the crack growth in the vicinity of the pin hole. A numerical method is performed to assess fatigue life of multi-row riveted metallic lap joint using a global/local FE model coupling approach [5] using standard AFGROW. The present work on a single-fastener metallic joint configuration is aimed to contribute to the work on Digital Twin which is a current research topic.

Also work has been conducted on estimation of fatigue life of these joints based on S–N life extensively. However, there is limited work on evaluating the health of these joints considering damage (crack) growth under fatigue loading with different bearing to bypass load ratios. This paper attempts to address the issues in computing the remaining life of these joints under different loading conditions, viz: constant amplitude and variable amplitude loading, respectively.

Constant amplitude block may not be representative of actual flight conditions [11]. Fighter aircraft loading standard for fatigue (FALSTAFF) simulates the loading spectra from actual flight records of wing-root loads from different fighter aircrafts on various missions [8]. Block-type loading is constructed from one mission and repeated to define a new sequence of load. Negative loads are filtered, and the data is normalised. In the variable amplitude loading, the challenge is to account for the number of cycles which is done in this paper by using rainflow cycle counting which reduces the spectrum into an equivalent set of simple stress levels. This is achieved by the four-point method [12]. Crack like damages which initiate and grow at critical locations of these joints affect the strength of the joint to a greater extend which if not monitored may lead to fracture. Crack growth analysis under the conditions mentioned above is conducted using Paris' Law with Elber correction for crack closure [4] where the useful life of these joints is computed at any given instance of loading.

2 Problem Definition

The geometry and configuration of fastener joint is shown in Fig. 1. Here, the 'L' is the length of plate, 'd' is the diameter of hole, 'e' is the distance between hole centre and right support and 't' is the thickness. The left end of the plate is subjected to a uniformly distributed load (UDL), and the right end is subjected to a constant displacement. This results in a total load of P_a at the left end and the bearing load of P_b at the pin and a bypass load of P_f. Aluminium 2024-T3 is the material of the plate. The material properties used in the analysis are listed in Table 1. The material is homogeneous and isotropic. The analysis is conducted on linear elastic material.

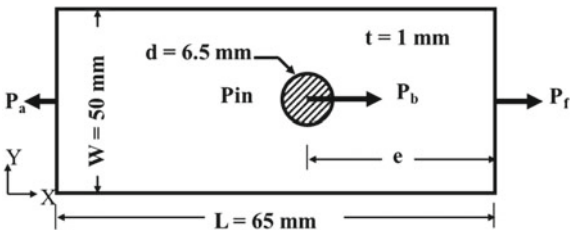

Fig. 1 Fastener joint configuration

Table 1 Material properties of plate [6]

Properties	Plate (Al 2024-T3)
E	72 GPa
v	0.3
σ_{yield}	324 MPa
K_{1C}	790 MPa $\sqrt{mm}$

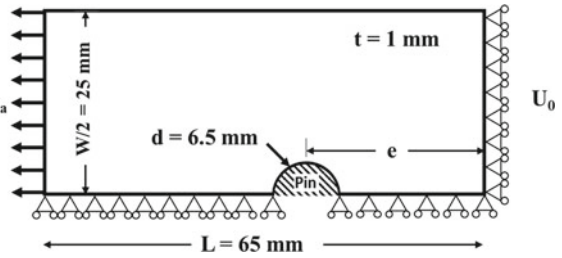

Fig. 2 Loads and boundary conditions in the model

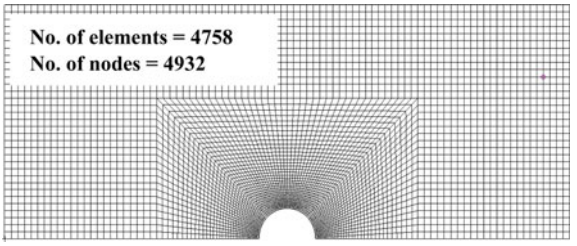

Fig. 3 FE model of the joint for configuration with e/L = 0.5

3 Methodology

3.1 FE Modelling

Numerical study of fastener joint is carried out using two-dimensional finite element analysis (FEA) with four-node quad elements using MSC NASTRAN [15] as the solver and post-processed in MSC PATRAN [16]. The boundary conditions of this configuration are shown in Fig. 2 along with the dimensions. The finite element mesh is arrived at after a convergence study with respect to bearing-bypass load ratio (Fig. 3). This mesh has 4758 elements and 4932 nodes. Since the model is symmetric about y-axis, a half-symmetry model is considered for analysis.

3.2 Damage Growth Study

Modified virtual crack closure integral (MVCCI) technique is used in estimating fracture parameters in crack growth studies and is shown pictorially in Fig. 4 and is given in Eqs. 1 and 2 [9, 10]. The elements near the crack tip are square elements. Crack growth life is estimated by Paris law with Elber correction [4] as given in Eq. 3. The constants in the equation are taken from literature [6].

$$G_I = \frac{1}{2\Delta A}[F_{xi}(U_x(i-1) - U_x(i-1)\prime)] \tag{1}$$

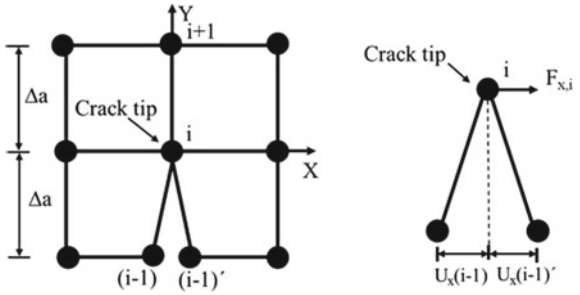

Fig. 4 MVCCI technique for a four-node quad element

$$K_I = \sqrt{\mathrm{G_I} * E} \tag{2}$$

where $\Delta A = \Delta a * b$, $\Delta a =$ elementlengthatcrackfront, $b =$ widthoftheelement

$$N_f = \int_{a_0}^{a_c} \frac{da}{C(\Delta K_{eff})^m} \tag{3}$$

where $K_{\min} = \left(a^{'} + b^{'} R\right) K_{\max}$, $K_{\max} = \sigma_{\max}\sqrt{\pi a_c}$, and $\Delta K_{\text{eff}} = K_{\max} - K_{\min}$

Here, $a^{'}$ and $b^{'}$ are crack growth material constants.

4 Results and Discussions

4.1 Stress Distribution Around Hole

Linear elastic analysis is conducted and the typical stress distribution for $e/L = 0.5$, $P_b/P_f = 0.61$, around the hole boundary is shown in Fig. 5.

4.2 Effect of Location of Hole on SCF

Stress concentration changes with the change in location of the hole. A study is conducted to see how the stress concentration factor (SCF) varies with respect to various locations of hole (e/L). SCF is computed by dividing tangential stress at 90° with nominal stress (Eq. 5). The nominal stress is defined in Eq. 4. The values of P_b/P_f (bearing-bypass ratio) and SCF for various locations of e/L are listed in Table 2. The variation of P_b/P_f is seen to be linear (Fig. 6).

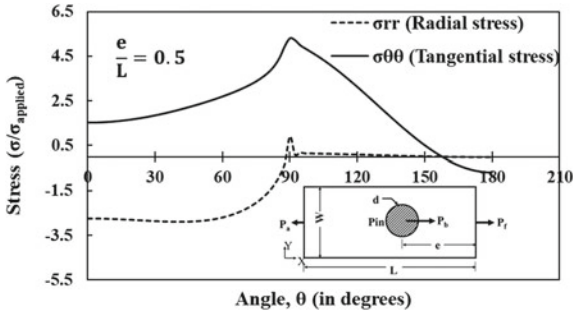

Fig. 5 Stress distribution around the hole

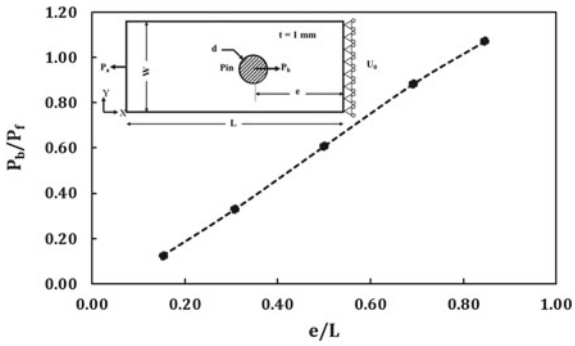

Fig. 6 Variation in bearing-bypass ratio with *e*/*L*

$$\sigma_{\text{nominal}} = \sigma_a \left(\frac{w}{w-d} \right) \tag{4}$$

$$\text{SCF} = \frac{\sigma_{\theta\theta}}{\sigma_{\text{nominal}}} \tag{5}$$

Table 2 Variation of P_b/P_f and SCF with *e*/*L*

e/*L*	P_b/P_f	SCF
0.15	0.12	2.88
0.31	0.33	3.81
0.50	0.61	4.61
0.69	0.88	5.11
0.85	1.07	5.10

4.3 *Effect of Bearing-Bypass Ratio on SCF*

Analysis is carried out by varying the P_b/P_f by varying the constant displacement imposed at the right end. The variation of SCF is plotted with respect to P_b/P_f and is compared with SCF from the previous section (Sect. 4.2) and is shown in Fig. 7. This shows that a bearing-bypass ratio can be chosen as an alternate in-place of location of hole (e/L) and gives similar stress distribution around the hole. Thus, the FEA due to change in the location of hole can be simulated by just varying the bearing-bypass ratio for affixed hole location. This reduces the need for separate finite element models for modelling fastener joint with holes at different locations. Three configurations have been considered as described in Table 3. Case 1 is considered to study when the entire load is bypassed to the right-side support. Case 2 is the typical configuration where some of the load is taken by the pin and rest is bypassed to the right support (Fig. 8). Case 3 is considered when all the load is taken by the pin and none of the load is bypassed. Any ratio of bearing-bypass load falls between those

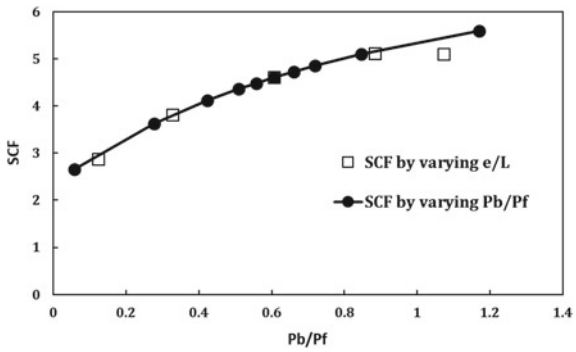

Fig. 7 Variation of SCF with bearing-bypass ratio

Table 3 Three cases considered for further study

Case No.	Boundary Condition
Case 1	Right support is present but the pin is removed
Case 2	Both pin and right support are present
Case 3	Pin is present and the right support is removed

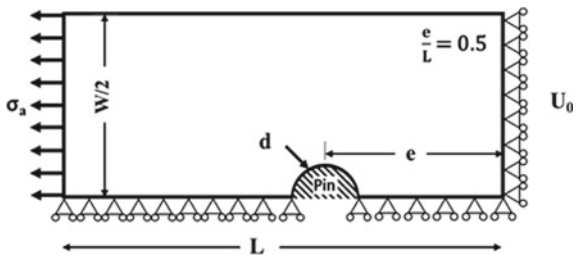

Fig. 8 Loads and boundary conditions for case 2

Table 4 SCF for two different configurations

	SCF	Tangential stress (MPa)
Case 2	4.61	338
Case 3	8.40	618

corresponding to case 1 and case 3. SCF for cases 2 and 3 are listed in Table 3 (Table 4).

4.4 Crack Growth Analysis

Crack growth analysis is conducted for various bearing-bypass ratios. The configuration of plate with crack is shown in Fig. 9. An initial crack of 1 mm is assumed to be present (following the damage tolerance procedure) at the critical location ($\theta = \pm 90°$) where the stress concentration is highest.

For the applied load (64 MPa), the stress intensity factor (SIF) for various crack sizes is plotted in Fig. 10 for two different bearing-bypass ratios. The configuration with higher bearing-bypass ratio has higher SIF. The difference between their SIF values narrows down as the crack grows farther from the hole. This is due to the

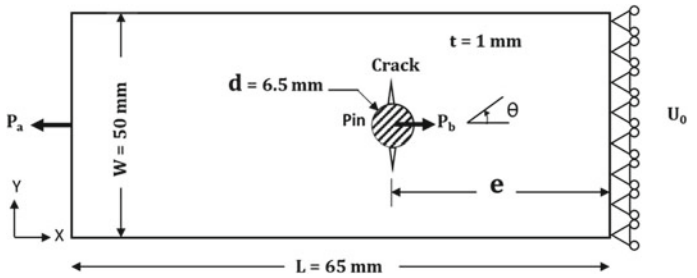

Fig. 9 Configuration of plate with crack

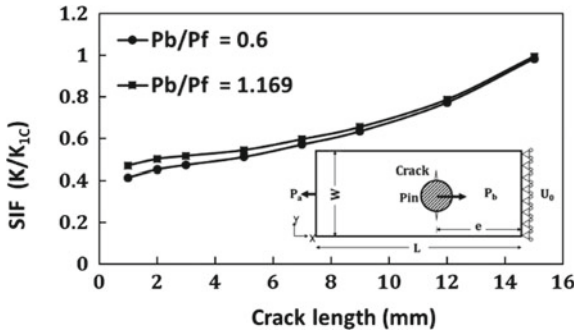

Fig. 10 SIF plots for two different bearing-bypass ratios

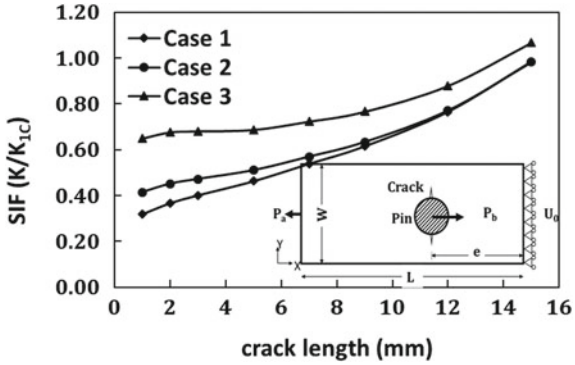

Fig. 11 SIF plots for three cases (Table 3)

reduced effect of bearing load in the region away from hole. So, the regions away from hole are more influenced by bypass load than bearing load. To examine this, the crack is modelled and SIFs are compared for the three cases as listed in Table 3. It can be noted that the highest SIF is for the presence of crack in case 3 where all the load is taken by the pin (Fig. 9). The lowest SIF is for case 1 where the whole load is bypassed to the support. Case 2 which corresponds to sharing of the load between the pin (bearing) and the support (bypass) lies in between the two. This shows that a configuration with any positive bearing-bypass ratio lies in between configurations corresponding to case 1 and case 3 (Fig. 11).

Crack growth studies are also conducted for two different bearing-bypass ratios and the number of cycles to failure is computed and is plotted in Figs. 12 and 13. It can be seen that for the crack at same location, bearing-bypass ratios can have a significant effect on crack growth life (Fig. 12). Crack propagation for the three cases mentioned (Table 3) is also computed and plotted in Fig. 13. It can be seen that in case 3 where the load is completely reacted by the pin, the crack growth life is approximately one-sixth of that when the complete load is bypassed to the support (case 1). Case 2 lies in between cases 1 and 3 as expected. This shows that the crack growth life is significantly affected by the bearing stress at the hole boundary.

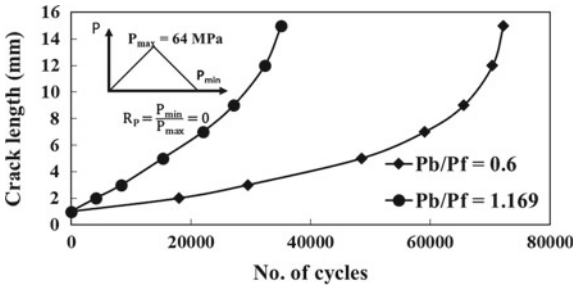

Fig. 12 Crack growth life for two ratios of bearing-bypass loading

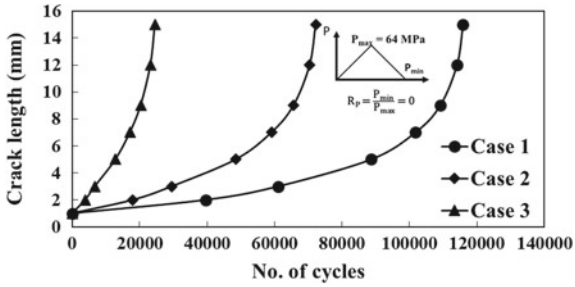

Fig. 13 Crack growth life for three cases

4.5 S–N Life

FF module (Fatigue and Fracture module) is a program that is developed in-house. FF module is used to compute S–N life. This program is written in Fortran 77. An algorithm is written for rainflow cycle counting. It uses the four-point rainflow cycle counting method to extract the cycles from a variable amplitude loading. 350 data points were taken from one mission profile from FALSTAFF load spectra and are constructed to form a load sequence. This generates 165 cycles from the rainflow cycle counting technique. This is applied as one block of loading (Fig. 14). The program has the options to apply multiple blocks of loading. The fatigue loading can be given as blocks of constant amplitude cycles, or multiple cycles of constant amplitude of different magnitudes or as a variable amplitude (as in the current work). The program computes the remaining life in blocks of loading till failure. Palmgren–Miners's rule (Eq. 6) is used for predicting the failure due to fatigue. Failure occurs when the Miner's index D reaches a value of 1.

$$D = \sum_{i=1}^{N} \frac{n_i}{N_i} \tag{6}$$

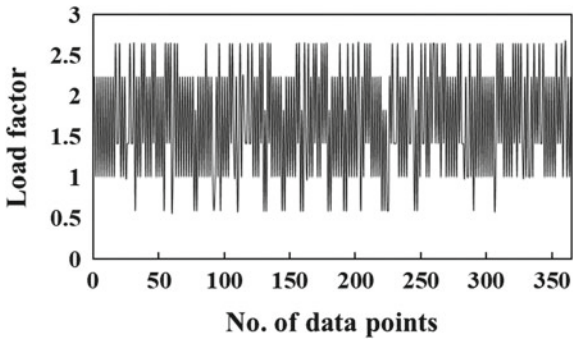

Fig. 14 One block of load

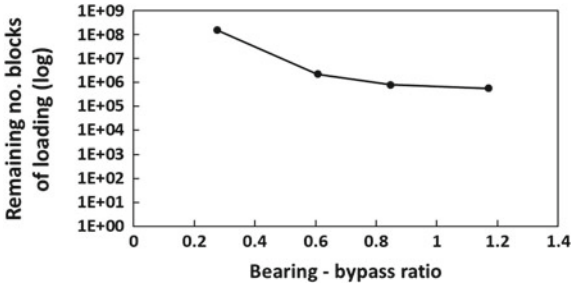

Fig. 15 Remaining life for various bearing-bypass ratios

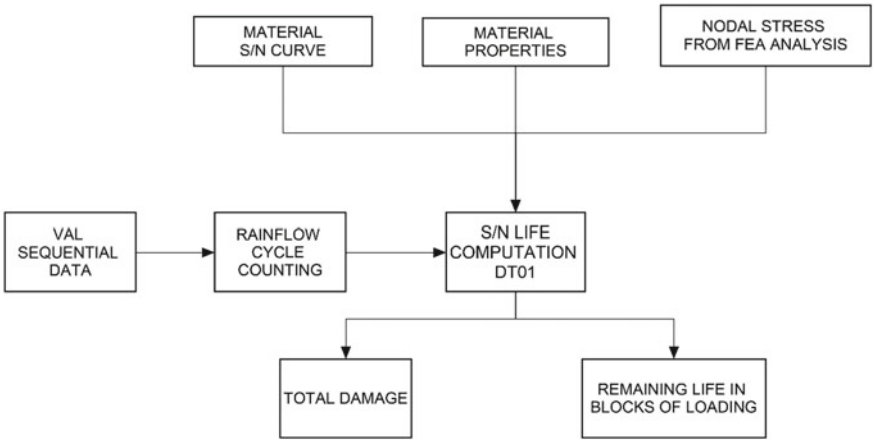

Fig. 16 Program flow chart showing the important steps

where n_i is the number of fatigue stress cycles of i type and N_i is the total number of cycles to failure of each of the i type fatigue cycles. A flowchart displaying the process of the program is shown in Fig. 15. Mean stress effects in fatigue are considered using Goodman relation. The remaining life for various bearing-bypass ratios is computed and shown in Fig. 15. It is seen that the remaining life of the joint varies significantly with respect to bearing-bypass load ratio. A flow chart depicting the important steps in the program is shown in Fig. 16.

5 Summary and Conclusions

- Two-dimensional, linear elastic finite element analysis of fastener joint is conducted using MSC PATRAN and MSC NASTRAN with four-node quad elements for different bearing-bypass load ratios.

- It is clearly seen that the effect of variation in stress due to position of hole can be simulated by varying the bearing-bypass load ratio in the finite element model with a fixed hole position, thus reducing the modelling and computational effort.
- Small allowable initial crack length is assumed at location of SCF, and the fracture parameters are computed by MVCCI. Cracks of smaller length are affected by the bearing stress near to the hole boundary compared to a longer crack.
- Crack growth life is estimated for various bearing-bypass load ratios. The remaining life is seen to decrease with increase in bearing-bypass load ratios.
- A computational program is used to compute the S–N life of the joint. An algorithm is written to extract the cycles from the variable amplitude load following the rainflow cycle counting method.
- There is a significant difference in S–N life for various bearing-bypass load ratios.

References

1. Broughton WR, Crocker LE, Grower MRL (2002) Design requirements for bonded and bolted composite structures. NPL Report MATC(A) 65
2. Crews JH, Jr, Naik RVA (1984) Failure analysis of a graphite/epoxy laminate subjected to bolt bearing loads. NASA Tech Memo 86297
3. Crews JH, Jr, Naik RVA (1986) Combined bearing and bypass loading on a graphite/epoxy laminate. NASA Tech Memo 87705
4. Elber W (1971) The significance of fatigue crack closure, In: damage tolerance in aircraft structure. ASTM, Phila (486):230–242
5. Li G, Renaud G, Liao M, Okada T, Machida S (2017) A methodology for assessing fatigue life of a countersunk riveted lap joint. Adv Aircr Spacecr Sci 4(1):1–19
6. Gomez MP, Ernst H, Vazquez H (1976) On the validity of Elber's results on fatigue crack closure for 2024-T3 aluminium. Int J Fract 12:178–180
7. Kabeel AM, Maimi P, Gonzalez EV, Gascons N (2015) Net-tension strength of double-lap joints under bearing-bypass loading conditions using the cohesive zone model, vol 119, pp 443–451
8. Manjunatha CM, Ranganath VR (2007) Prediction of optimum spectrum for full scale fatigue test. In: 15th national seminar on aerospace structures, Coimbatore, Tamil Nadu, India, pp 15–16
9. Ramamurthy TS, Krishnamurthy T, Badrinarayana K, Vijaykumar K, Dattaguru B (1986) Modified crack closure integral method with quarter point elements. Mech Res Commun 13(4):179–186
10. Rybicki EF, Kanninnen MF (1977) A finite element calculation of stress intensity factors by a modified crack closure integral. Eng Fract Mech 9(4):931–938
11. Ward-Close CM. (1983) Simulated flight (Falstaff) fatigue crack growth in titanium alloy Ti-4A1-4Mo-2Sn-0.5Si. RAE Technical Report No 83056
12. Lee Y-L, Rjhung T (2012) Rainflow cycle counting techniques, metal fatigue analysis handbook. In: Practical problem-solving techniques for computer-aided engineering, pp 89–114
13. Whitman ZL (2012) The effect of fatigue cracks on fastener flexibilty, load distributration, and fatigue crack growth. Ph.D. thesis
14. Zhang Z, Wang W, Rans C, Benedictus R (2016) An experimental investigation into pin loading effects on fatigue crack growth in fiber metal laminates. In: Proceedia structural integrity 2, 21st European conference on fracture, ECF21, pp 3361–3368

15. The MSC NASTRAN documentation (2017) MSC Software Corporation, Macarthur Court, Newport Beach-CA, USA, 4675